Multidrug Resistance Reversal Effects of Aminated Thioxanthones and Interaction with Cytochrome P450 3A4

Andreia Palmeira[1,2,3], Emília Sousa[1,2], Miguel X. Fernandes[4], Madalena M. Pinto[1,2], M. Helena Vasconcelos[3,5]

[1] Departamento de Química, Laboratório de Química Orgânica e Farmacêutica, Faculdade de Farmácia, Universidade do Porto, Rua Anibal Cunha, Porto, Portugal.
[2] Centro de Química Medicinal – Universidade do Porto (CEQUIMED-UP).
[3] Cancer Drug Resistance Group, IPATIMUP – Institute of Molecular Pathology and Immunology of the University of Porto, Rua Dr Roberto Frias, Porto, Portugal.
[4] Centro de Química da Madeira, Universidade da Madeira, Campus da Penteada, Funchal, Portugal.
[5] Departamento de Ciências Biológicas, Laboratório de Microbiologia, Faculdade de Farmácia, Universidade do Porto, Rua Anibal Cunha, Porto, Portugal.

Received, September 12, 2011; Revised, November 9, 2011; Accepted, November 30, 2011; Published, December 5, 2011.

ABSTRACT - Purpose. Aminated thioxanthones have recently been described as dual-acting agents: growth inhibitors of leukemia cell lines and P-glycoprotein (P-gp) inhibitors. To evaluate the selectivity profile of thioxanthones as inhibitors of multidrug resistance (MDR), their interaction with other ABC transporters, which were found to have a strong correlation with multidrug resistance, such as multidrug resistant proteins 1 (MRP1), 2 (MRP2) and 3 (MRP3) and breast cancer resistance protein (BCRP) was also evaluated. The interaction of thioxanthones with cytochrome P450 3A4 (CYP3A4) together with the prediction of their binding conformations and metabolism sites was also investigated. **Methods**. The UIC2 monoclonal antibody-labelling assay was performed using P-gp overexpressing leukemia cells, K562Dox, incubated with eight thioxanthonic derivatives, in order to confirm their P-gp inhibitory activity. A colorimetric-based ATPase assay using membrane vesicles from mammalian cells overexpressing a selected human ABC transporter protein (P-gp, MRP1, MRP2, MRP3, or BCRP) was performed. To verify if some of the thioxanthonic derivatives were substrates or inhibitors of CYP3A4, a luciferin-based luminescence assay was performed. Finally, the *in silico* prediction of the most probable metabolism sites and docking studies of thioxanthones on CYP3A4 binding site were investigated. **Results**. Thioxanthones interacted not only with P-gp but also with MRP and BCRP transporters. These compounds also interfere with CYP3A4 activity *in vitro*, in accordance with the *in silico* prediction. **Conclusion**. Thioxanthonic derivatives are multi-target compounds. A better characterization of the interactions of these compounds with classical resistance mechanisms may possibly identify improved treatment applications.

INTRODUCTION

Cancer is a major health concern worldwide and the emergence of cell populations resistant to multidrug-based chemotherapy constitutes a major obstacle to treatment (1). Multidrug resistance (MDR) involves cellular resistance to several structurally unrelated drugs and one of the possible reasons is the overexpression of ATP-binding cassette (ABC) transporters (2). These transporters pump the antitumor agents to the extracellular medium, removing them from the site of action, thereby rendering the treatment ineffective (3). The first ABC transporter whose overexpression was shown to confer a MDR phenotype was P-glycoprotein (P-gp), the product of the *mdr1* (ABCB1) gene (4). P-gp transports neutral or positively-charged hydrophobic substrates, particularly anticancer drugs, consuming energy from ATP hydrolysis (1).

Drug discovery in the last century has largely been based on the concept of "one molecule – one target – one disease" but more recently there has been a growing recognition that molecules that modulate multiple targets simultaneously can be beneficial for treating several diseases (5).

The biological interest in thioxanthones started with the use of lucanthone and hycanthone as antischistosomal agents. However, their ability to intercalate into DNA (6) prompted these compounds to be used as promising antitumor agents.

Corresponding Authors: Emília Sousa and M. Helena Vasconcelos, Faculdade de Farmácia, Universidade do Porto, Rua Anibal Cunha, Porto, Portugal; Email: esousa@ff.up.pt, hvasconcelos@ipatimup.pt

The similarities of these compounds with other intercalating agents lay on the tricyclic moiety and the aminated side chain (6). However, their mutagenicity (which was associated with the presence of the methylene moiety directly linked to C-4 (7)) proscribed their use in cancer chemotherapy. SR 233377 and SSR271425, two more recent aminated thioxanthones, entered phase I clinical trials (8,9) but were found to cause cardiotoxicity. Therefore, it is of considerable importance to further investigate aminated thioxanthonic derivatives, in the search for more active and less toxic antitumor compounds.

We have previously shown that aminated thioxanthones may be dual-acting agents capable of simultaneously inhibiting cell growth and P-gp function (10). These compounds resulted from the hybridization between a thioxanthonic scaffold (described for its antitumor activity) (9,11) and pharmacophoric features for P-gp inhibition (an amine group) (12). Overall, results with a leukemia cell line (P-gp overexpressing) resistant to doxorubicin, showed that aminated thioxanthones (**1**-**8**, Figure 1) can be characterized as a new class of P-gp inhibitors with improved efficacy when compared to verapamil, a known P-gp inhibitor (10).

However, before proceeding to *in vivo* studies or to a new round of synthesis, the evaluation of the direct interaction of thioxanthones with P-gp and interaction with other drug transporters, or metabolizing enzymes, is necessary. In fact, as data regarding the role of P-gp in drug resistance accumulated, it became clear that other transporters could confer resistance to cytotoxic agents. The multidrug-resistance associated transporter 1 (MRP1 or ABCC1), MRP2 (or ABCC2, cMOAT) and MRP3 (or ABCC3) as well as the breast cancer associated protein (BCRP or ABCG2, MXR) are also examples of transporters implicated in MDR (13).

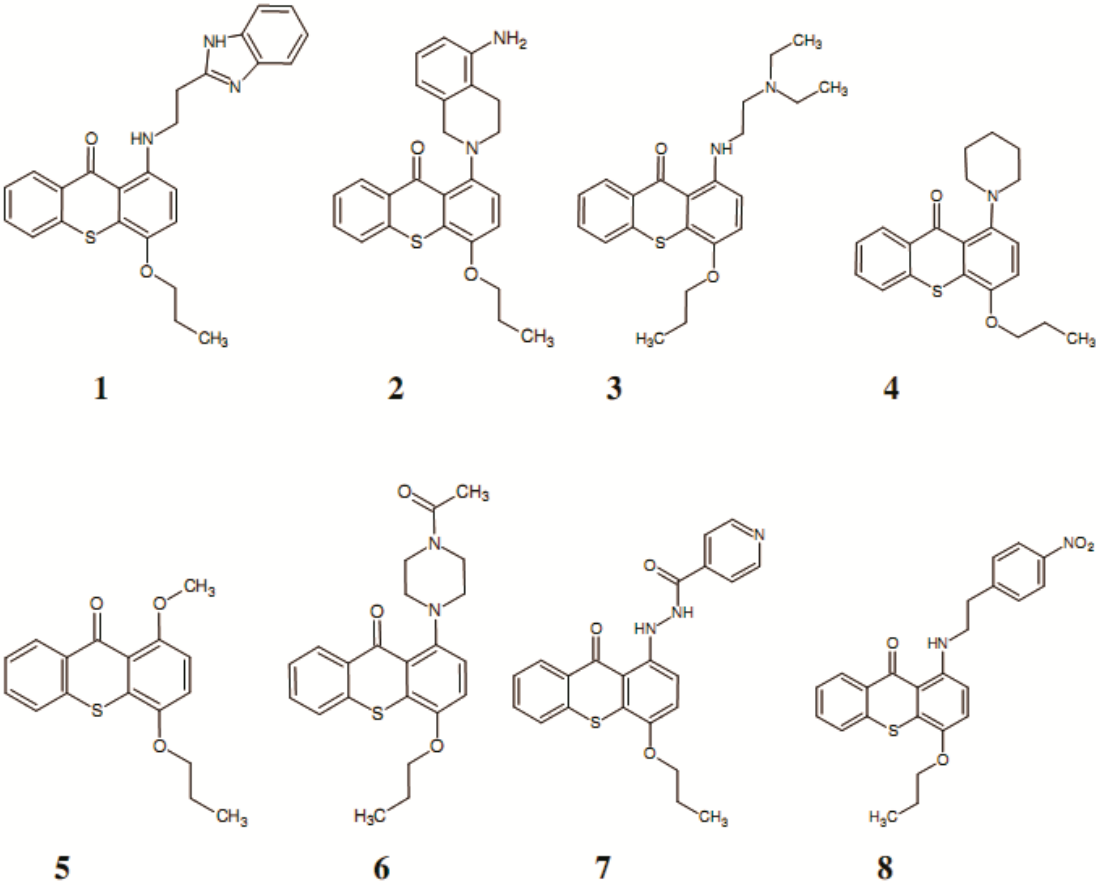

Figure 1. Thioxanthonic derivatives **1**-**8** described as dual P-gp and cell growth inhibitors (10): 1-[2-(1*H*-benzimidazol-2-yl)ethanamine]-4-propoxy-9*H*-thioxanthen-9-one (**1**), 1-(5-amino-3,4-dihydroisoquinolin-2(1*H*)-yl)-4-propoxy-9*H*-thioxanthen-9-one (**2**), 1-{[2-(diethylamino)ethyl]amino}-4-propoxy-9*H*-thioxanthen-9-one (**3**), 1-(piperidin-1-yl)-4-propoxy-9*H*-thioxanthen-9-one (**4**), 1-methoxy-4-propoxy-9*H*-thioxanthen-9-one (**5**), 1-(4-acetylpiperazin-1-yl)-4-propoxy-9*H*-thioxanthen-9-one (**6**), *N*'-(9-oxo-4-propoxy-9*H*-thioxanthen-1-yl)pyridine-4-carbohydrazide (**7**) and 1-{[2-(4-nitrophenyl)ethyl]amino}-4-propoxy-9*H*-thioxanthen-9-one (**8**).

Indeed, an issue that affects all generations of P-gp inhibitors concerns their multiple actions towards various ABC transporters. Even the most recent and potent P-gp inhibitors such as tariquidar (14) (P-gp and BCRP inhibitor) and CBT-1 (15) (P-gp and MRP1 inhibitor) modulate more than one ABC transporter, and both have entered clinical trials. It is not surprising to find compounds which are multi-target inhibitors of ABC transporters, since these proteins share structural and functional similarity (16). Indeed, since the clinical MDR appears to be related to the overexpression of several transporters, compounds that inhibit multiple ABC transporters may possibly be preferable to the use of a combination of specific modulators, as they would reduce cumulative toxicities and drug–drug interaction (17-19).

One of the main issues regarding second generation P-gp inhibitors was the pharmacokinetic interactions due to overlapping substrate specificity between P-gp and cytochrome P450, which required an increase in the dose of the cytotoxic drug in order to achieve therapeutic efficacy (20).

The novelty of this work resides in the investigation of several potential targets of newly synthesized thioxanthonic derivatives. The aim was to better characterize the P-gp inhibitory activity of thioxanthones and to further explore the potential of interaction with other ABC transporters and CYP3A4, as the selectivity profile of these compounds may help to clarify their possible clinical usefulness. Finally, a computational prediction of the docking conformations of thioxanthones on CYP3A4 as well as the most probable metabolism sites was also performed.

METHODS

Chemicals

The MDR1 UIC2 shift assay was purchased from Millipore (ECM905, Madrid, Spain). The BCRP ATPase kit (SB BCRP HAM Sf9 PREDEASY™ ATPase Kit), BCRP—deficient ATPase control kit (SB defBCRP HAM Sf9 PREDEASY™ Ctrl Kit), MDR1 ATPase kit (SB MDR1/P-gp PREDEASY™ ATPase Kit), MDR1-deficient control Kit (SB defPgp PREDEASY™ CTRL Kit), MRP1 (SB MRP1 PREDEASY™ ATPase Kit), MRP2 (SB MRP2 PREDEASY™ ATPase Kit) and MRP3 (SB MRP3 PREDEASY™ ATPase Kit) ATPase kits and MRP-deficient control kit (SB defMRP PREDEASY™ CTRL Kit) were purchased from SOLVO Biotechnology (Budapest, Hungary). In addition, the P450-Glo kit (V9800) and NADPH regeneration system (V9510) were purchased from Promega (Madison, USA). D-Luciferin (L9504) and CYP3A4 microsomes (C4982) were purchased from Sigma Aldrich (St. Louis, USA). Synthesis of compounds **1-8** was performed according to the described procedure (10).

MDR1 UIC2 shift assay

The MDR1 UIC2 shift assay was performed using P-gp overexpressing leukemia cells, K562Dox, as previously described (21) with minor modifications. K562Dox is a cell line derived from K562 by doxorubicin stimulated overexpression of P-gp (kindly donated by Prof. J.P. Marie, Paris, France). P-gp expression on the K562Dox cell line (by Western blot) has previously been confirmed (22). K562Dox cells were washed with phosphate buffered saline (PBS) and re-suspended in UIC2 binding buffer (PBS + 1% BSA). Approximately 1×10^6 cells in 800 µL binding buffer were pre-warmed at 37ºC for 10 min, incubated with the compounds **1-8** (final concentration 200 µM) or Na_3VO_4 (final concentration of 20 µM; positive control, noncompetitive inhibitor), verapamil, quinidine, and mibefradil (final concentration of 200 µM; negative control, competitive inhibitors) at 37ºC for 30 min, and the monoclonal antibody UIC2 was added (final concentration 12.5 $\mu g.mL^{-1}$). After 30 min at 37ºC, 800 µL of ice-cold UIC2 buffer was added to stop the reaction. Cell samples were washed with cold buffer twice, re-suspended in 500 µL ice-cold UIC2 buffer and goat anti-mouse IgG2a-phycoerithrin (PE) was added (final concentration of 5 $\mu g.mL^{-1}$). After 45 min at 4ºC in the dark, samples were washed twice using UIC2 ice-cold buffer and finally re-suspended in 250 µL ice-cold UIC2 binding buffer containing propidium iodide (final concentration of 40 $\mu g.mL^{-1}$). The cellular suspension was analyzed using a flow cytometer (Epics XL-MCL, Beckman Coulter, USA) and FL2 and FL3 channels were used for indirect UIC2 staining and dead cell exclusion by propidium iodide, respectively. At least 5000-10000 events were collected. Fluorescence intensity associated with the cells was expressed on a log scale. Normal mouse immunoglobulin G2a (IgG2a) served as a negative control. Results are presented as the average of at least three independent experiments. Fluorescence intensity ratio ($FL2_{ratio}$) was calculated in relation to the DMSO solvent control (cells treated with DMSO and medium only, and incubated with primary and secondary antibodies as described). It was calculated using the following formula that fits

the blank control to zero for easier interpretation: $FI2_{ratio} = (FI_{test} - FI_{dmso}).FI_{dmso}^{-1}$.

ATPase activity assays

ATPase activity was measured according to the described procedure (23). The predeasy MDR1-ATPase kit, BCRP-HAM-ATPase kit, MRP1, MRP2 and MRP3 ATPase kits were used for determining the effect of compounds **1** and **2** on the MDR1-, BCRP-, MRP1-, MRP2- and MRP3-ATPase activities respectively, according to the manufacturer's instructions. In brief, membrane vesicles in TMEP solution (50 mM Tris, 50 mM mannitol, 2 mM ethylene glycol tetraacetic acid (EGTA), 8 $\mu g.mL^{-1}$ aprotinin, 10 $\mu g.mL^{-1}$ leupeptin, 50 $\mu g.mL^{-1}$ phenylmethanesulfonylfluoride (PMSF), 2 mM dithiothreitol (DTT), pH 7.0) were incubated at a concentration of 20 µg per well with an assay mix (40 mM 3-morpholinopropanesulfonic acid with (MRP assay) or without glutathione (the remaining assays)), 5 mM ATP and four concentrations of test compounds **1** and **2** (1.6, 8.0, 40.0, 200.0 µM). Two protocols were used: (a) incubation with or without 1.2 mM Na_3VO_4 (activation study) or (b) incubation with 200.0 µM of a known substrate (verapamil for MDR1 assay, *N*-ethylmaleimide glutathione (NEM-GS) for MRP1 assay, sulfasalazine for MRP2 and BCRP assay, and benzbromarone for MRP3 assay) and with or without 1.2 mM sodium orthovanadate (inhibition study), for 10 min at 37°C. Controls without treatment and with a control inhibitor at 40.0 µM (cyclosporine A for MDR1 and MRP3 assay, benzbromarone for MRP1 and MRP2, and Hoechst 33342 for BCRP assay) were also used. The reaction was stopped by adding a developer solution (ethanol 95%) to each well, followed by a blocker solution (4 mM sodium azide) and an additional 30 min incubation at 37ºC. Optical density (OD) was read at 630nm. The amount of phosphate (Pi) liberated by the transporter is proportional to the activity of the transporter (24). Transporter activity was measured as the vanadate sensitive portion of total ATPase activity required to eliminate background ATPase activity (25). Liberated Pi was quantified based on the calibration line established with Pi standards (0, 4, 8 nmol per well). Results are presented as % of control (% of the nontreated control). The IC_{50} concentrations were calculated from the inhibition studies. Similar assays were also performed using the predeasy defMDR1, defBCRPHAM and defMRP ATPase control kits, using the manufacturer protocols (a).

CYP3A4 interaction assay

Eight thioxanthonic derivatives (**1-8**) were screened for interference with CYP3A4 using the CY3A4 P450-Glo assay (Promega, Madison, USA) following the manufacturer's instructions. In brief, recombinant CYP3A4, 1 pmol/well, was pre-incubated for 10 min at 37ºC with 50 µM luciferin-6'-benzyl ether (luciferin-BE) and 200 µM of each thioxanthone. The reaction was initiated upon the addition of 25.0 µL of the NADPH regenerating solution (1.3 mM $NADP^+$, 3.3 mM glucose-6-phosphate; $4U.ml^{-1}$ glucose-6-phosphate dehydrogenase; Promega, Madison, USA). Following 30 min incubation at 37ºC, 50.0 µL of the detection reagent containing a recombinant, stable luciferase was added. The resulting luminescence was measured after 20 min incubation at room temperature. Controls without compound or with a known CYP3A4 inhibitor, ketoconazole (200 µM), were also used.

The IC_{50} value (concentration that inhibits the metabolism of the known substrate luciferin-BE by 50%) of compounds **1** and **2** was determined with the same protocol but testing eight concentrations of **1** and **2** ranging from 2 nM to 200 µM (0.002, 0.013, 0.064, 0.32, 1.60, 8.00, 20.00, and 200.00 µM). The IC_{50} value was calculated after scaling the data to 100% activity.

Modelling the metabolism of compounds 1 and 2

All calculations were performed on a commodity PC Microsoft Windows 7 with an Intel(R) Core(TM) i5 processor. Compounds **1-8** were drawn and minimized using the AM1 semi-empirical method (Hyperchem v8.07, Hypercube, USA) (26).

Compounds **1** and **2** were submitted to the MetaSite v3.0.4 program (MolDiscovery, Middlesex, United Kingdom) (27) which is a fully automated procedure that considers structural complementarity between the enzyme active site and ligand and provides the best orientation. Both the protein active site and ligand are represented by selected distance-based descriptors using molecular interaction fields computed in GRID. Metabolism site prediction was performed for CYP3A4. The most probable sites of metabolism (SOM) or "hot spots" were plotted according to their scores. The metabolism site is described by a probability index which is a product of similarity between ligand and protein. In this study, the top six averaged rankings with the reactivity component were considered. SOM was used to calculate those atoms that contribute most to orienting the metabolism site towards the heme group.

Furthermore, compounds **1**-**8**, ketoconazole (known CYP3A4 inhibitor) (28) and propofol (compound not metabolized by CYP3A but by CYP2B6) (29) were docked into CYP3A4 (pdb code: *2V0M*; human CYP3A4 with crystallographic ketoconazole) by means of Autodock Vina embedded in PyRx.v3.2 software (30) (Molecular Graphics Lab, La Jolla, CA, USA). Exhaustiveness of eight was followed and the box size used was 20 × 20 × 20 Å, centred on the crystallographic ligand coordinates.

STATISTICAL ANALYSIS

Data was expressed as the mean ± SE of at least three independent experiments, except in the case of vanadate-sensitive ATPase activity (mean of two experiments only) and analyzed by the Student's *t* test. *P*-values below 0.05 were considered statistically significant when data was analysed for statistical meaningfulness (student's *t* test).

RESULTS

MDR1 UIC2 shift assay

In an effort to confirm the previously-found direct interaction of thioxanthones **1**-**8** with P-gp (10), a MDR1 UIC2 shift assay was performed (Figure 2). Therefore, two competitive inhibitors (**2** and **3**) and six noncompetitive inhibitors (**1**, **4**-**8**) were selected from our previous work to perform the MDR1 shift assay. This assay uses the monoclonal antibody (mAb) UIC2, a conformation-sensitive antibody which preferentially binds to an external epitope of P-gp which is in the process of substrate transportation (31,32). UIC2 is also unique among the mAbs directed against P-gp because it blocks drug pumping efficiently, probably by trapping P-gp in a certain conformational state of its enzymatic cycle (32). Based on this conformation-sensitive competition assay, it is possible to distinguish between compounds that are being transported (substrates or competitive inhibitors) from compounds that block the P-gp transportation cycle (noncompetitive inhibitors) (33). Figure 2 shows that mibefradil, verapamil and quinidine (all P-gp substrates used as controls) increased UIC2 labelling of K562Dox cells, as expected. The blocking of the ATP site by sodium vanadate decreased UIC2 labelling, also as expected. Compounds **1**, **4**, **6**-**8** had UIC2 binding reactivity inferior to the DMSO control while compound **2** had a UIC2 binding reactivity greater than that of the DMSO control (Figure 2).

ATPase assay

As our previous data showed that compounds **1** and **2** were the most potent P-gp noncompetitive and competitive inhibitors, respectively (10), they were further investigated with ATPase screening assays for various ABC transporters (including P-gp), which are based on purified membrane vesicles from mammalian cells overexpressing a selected human ABC transporter protein. The transport function of ABC transporters is tightly coupled to its ATPase activity, as ATP hydrolysis drives the transport process (34). Substrates transported by P-gp can therefore be detected by hydrolysis of ATP and production of the inorganic phosphate detected by a colorimetric reaction (35). The assay is composed of two different tests: an activation and inhibition test, both of which are complementary assays. The assay is a modification of the method of Sarkadi *et al* (36). In the activation test, the transported substrates increase baseline vanadate sensitive ATPase activity while inhibitors decrease the baseline vanadate sensitive ATPase activity. A stimulation detected on the activation assay indicates that the compound is a substrate of the transporter being studied. In the inhibition test, carried out in the presence of a known substrate/activator (which varies according to the ABC transporter under study), inhibitors or transported compounds inhibit the maximum vanadate sensitive ATPase activity (37). Interactions detected in the inhibition test indicate interactions of the test compounds with the transporter. The obtained results are graphically represented in Figures 3 and 4 and the IC_{50} values are indicated in Table 1. Compounds **1** and **2** did not affect levels of Pi liberation on membranes lacking P-gp, BCRP, or MRP (results not shown).

CYP3A4 interaction assay

Luciferin-BE is used as a CYP3A4 substrate which is converted by the enzyme to luciferin product, which in turn reacts with luciferase to produce an intensity of light proportional to CYP activity (38). Changes in the luminescence signals from samples treated with test compound compared to untreated control samples, represent modulation of CYP3A4 activity by the test compound (39).

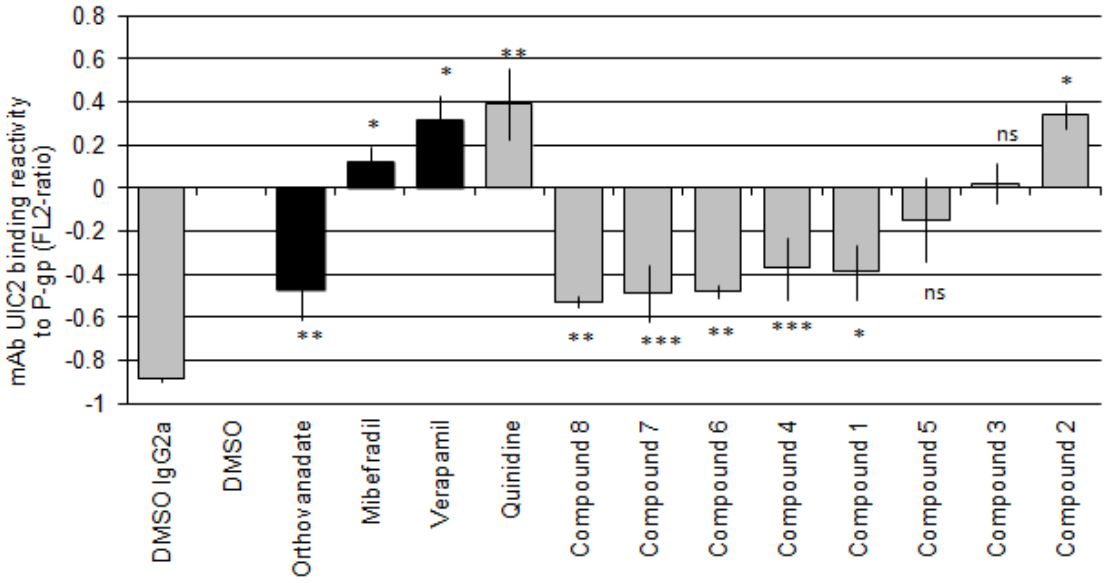

Figure 2. Effect of eight thioxanthonic derivatives on mAb UIC2 binding reactivity to P-gp, presented as a FL2-ratio. Normal IgG2a was used as negative control. Control luminescence (DMSO) is represented as zero for easier interpretation. An FL2-ratio less than zero corresponds to inhibitors of the P-gp transportation cycle, i.e., noncompetitive P-gp inhibitors. An FL2-ratio greater than zero corresponds to compounds that stimulate the P-gp transportation cycle i.e., substrates of P-gp or competitive P-gp inhibitors. Results are expressed as the mean ± SE of at least three independent experiments. Na_3VO_4, verapamil, mibefradil and quinidine were used as controls. Statistical significance was tested by the paired *t*-test using DMSO as control. *** indicates $P < 0.001$; ** indicates $0.001 < P \leq 0.01$; * indicates $0.01 < P \leq 0.05$. ns indicates not significant, i.e., $P > 0.05$ (n=4).

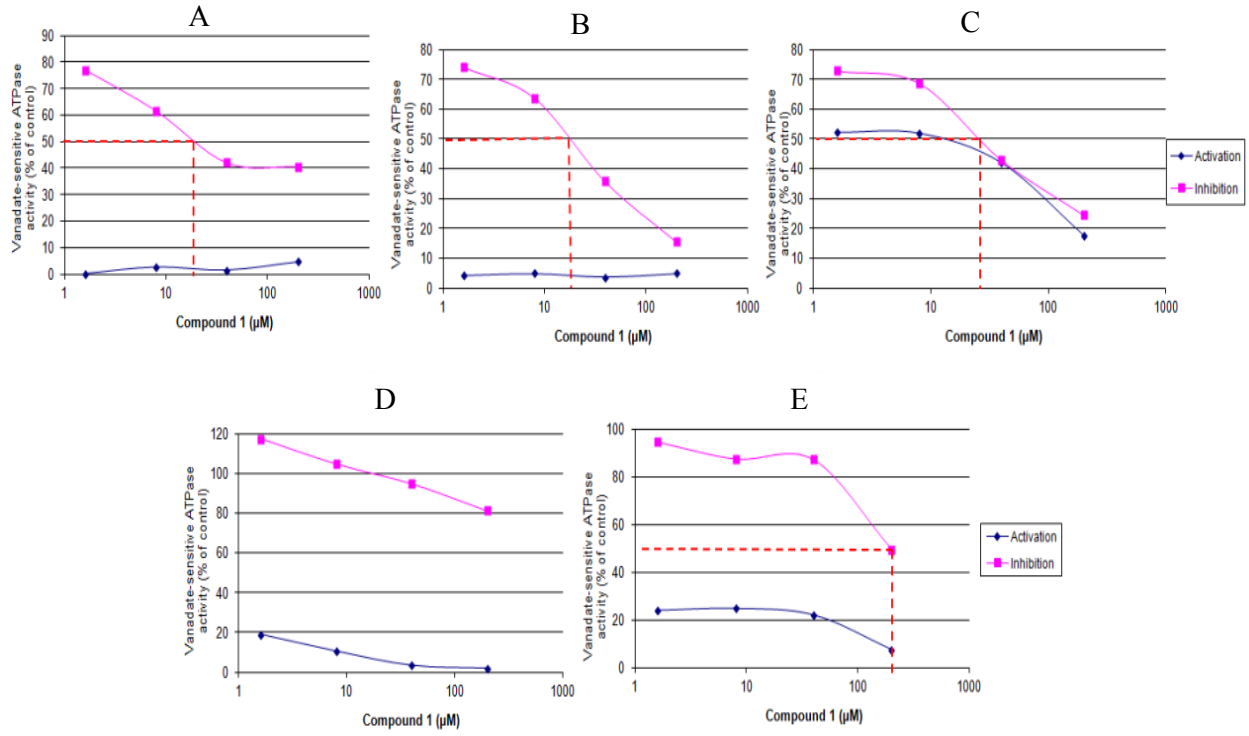

Figure 3. Vanadate-sensitive ATPase activity (plotted as % of non-treated control in nmol Pi.mg protein^{-1}.min^{-1}) of P-gp (A), BCRP (B), MRP1 (C), MRP2 (D) and MRP3 (E) membrane preparations in the presence of compound **1** alone (activation assay) or in combination with a substrate (inhibition assay) at different concentrations (1.6, 8.0, 40.0, 200.0 μM). Results represent the average of two independent experiments performed in duplicate. IC_{50} values are represented with the broken line.

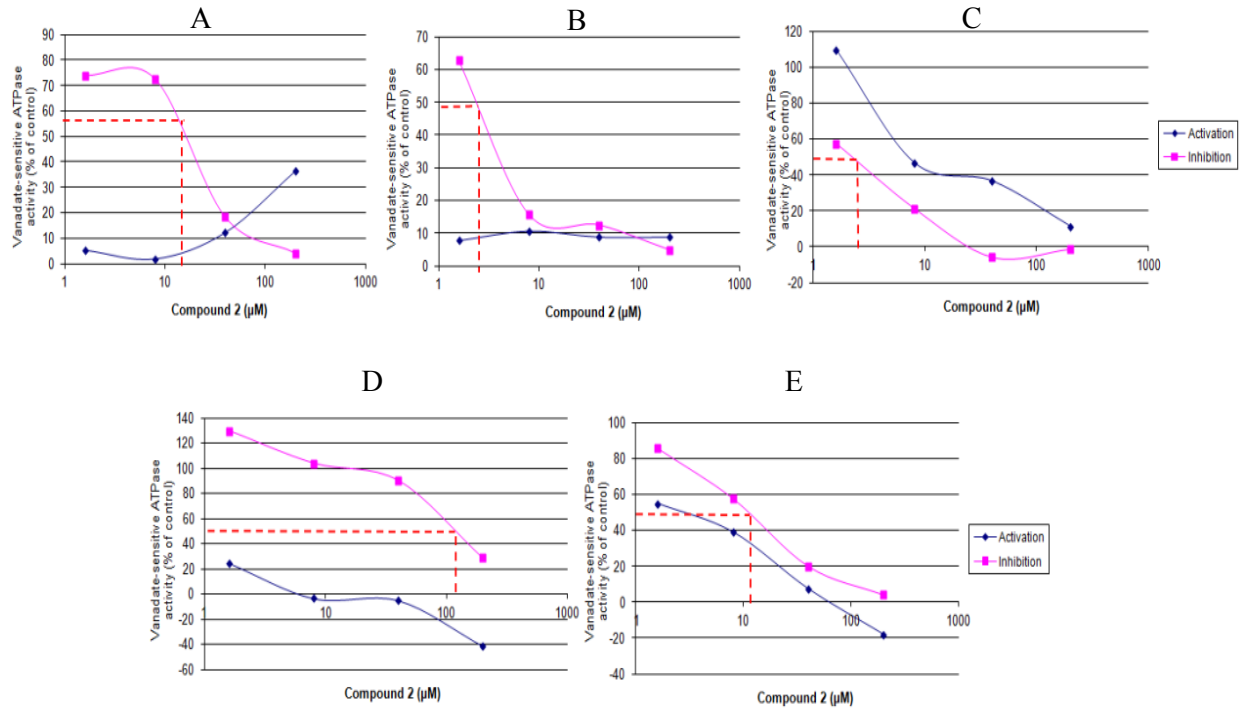

Figure 4. Vanadate-sensitive ATPase activity (plotted as a % of non-treated control) in nmol Pi.mg protein^{-1}.min^{-1}) of P-gp (A), BCRP (B), MRP1 (C), MRP2 (D) and MRP3 (E) membrane preparations in the presence of compound **2** alone (activation assay) or in combination a substrate (inhibition assay) at different concentrations (1.6, 8.0, 40.0, 200.0 μM). Results represent the average of two independent experiments performed in duplicate. IC_{50} values are represented with the broken line.

Table 1. ATPase inhibitory effect of compounds **1** and **2** in the presence of known substrates of several ABC transporters

IC_{50} (μM)	P-gp	BCRP	MRP1	MRP2	MRP3
Compound 1	20	20	25	> 200	200
Compound 2	20	2	4	145	13

Results represent the average of two independent experiments performed as duplicates.

Figure 5 shows that the eight thioxanthonic derivatives (**1**-**8**) interfere with CYP3A4 activity (inhibitors or substrates) as they decreased the levels of luciferin-associated luminescence when tested at concentrations of 200 μM.

To calculate the CYP3A4 IC_{50} of our best P-gp inhibitors, the same luciferin luminescence-based assay was used to test several concentrations of compounds **1** and **2** (Figure 6). It was found that these compounds presented IC_{50} values for CYP3A4 inhibition of approximately 1-2 μM (Figure 6). The CYP3A4 inhibition is low for compounds **1** and **2** at concentrations below 0.01 μM, but is almost total for concentrations close to 100 μM.

Modelling the metabolism of compounds 1 and 2

In view of these results, *in silico* analysis of the potential metabolism sites on the thioxanthonic derivatives **1** and **2** was performed. The metabolism site and molecular contribution to the exposure of a reactive atom to the heme moiety (activity contribution plot) were determined by MetaSite (40). The program has been described as being capable of predicting the most probable metabolism site within the top three predictions in 80% of the cases in structurally diverse compounds (27). MetaSite predicted that the methylene groups directly linked to the aniline at C-1 in compounds **1** and **2** were the top-ranked metabolism sites by CYP3A4 (Figure 7, dark red arrows). Other possible metabolism sites are also depicted in Figure 7 (light red arrows).

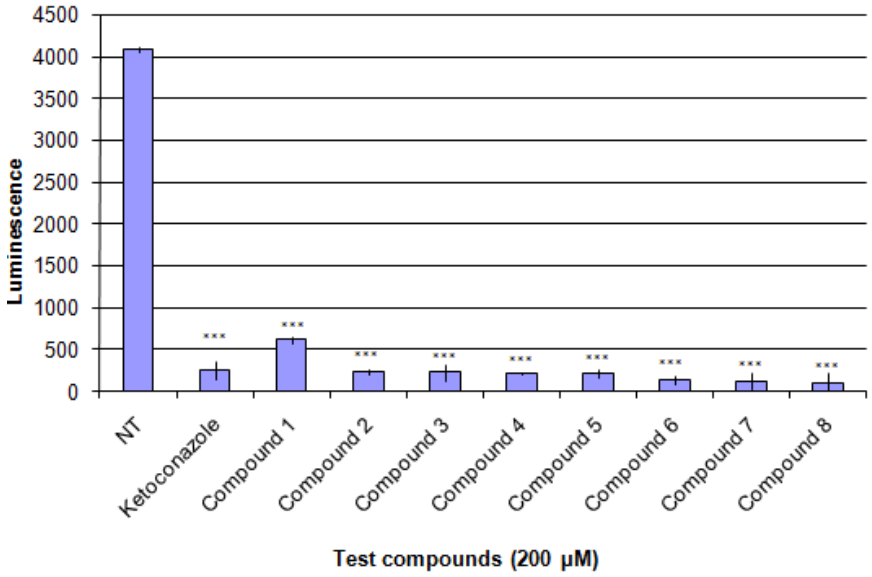

Figure 5. CYP3A4 inhibition assay. % of RLU in relation to the non-treated (NT) control was used to assay the potential of the thioxanthonic derivatives for interaction with CYP3A4. Reactions were performed using 1pmol recombinant CYP3A4 in 10 min reactions at 37ºC with 2 µM of luciferin-BE as substrate, in combination with 200 µM of a positive control (a known CYP3A4 inhibitor, ketoconazole) or 200 µM of the test thioxanthonic derivatives **1-8**. Values are means ± SE of three independent experiments. Statistical significance was tested through the paired *t*-test using the non-treated cells (NT) as control. *** indicates $P < 0.001$ (n=3).

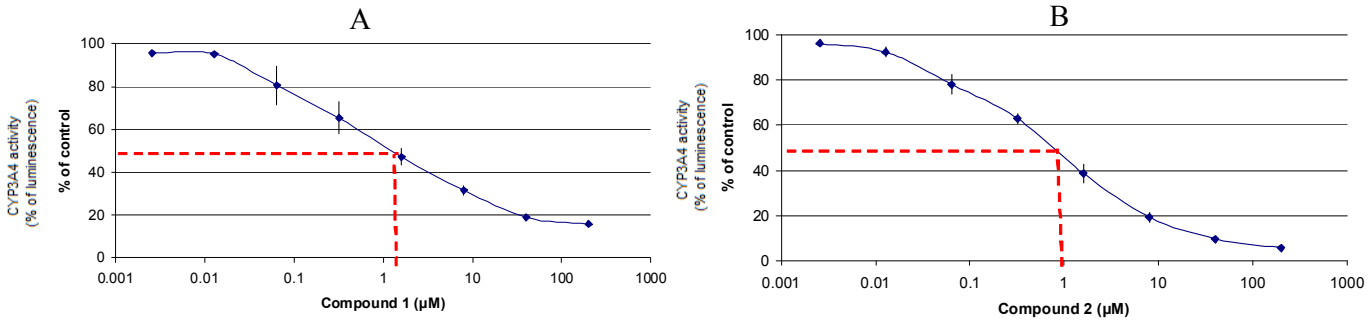

Figure 6. CYP3A4 inhibition assay. % of RLU in relation to the non-treated (NT) control was used to analyse the potential of compound **1** (A) and compound **2** (B) to inhibit CYP3A4. Reactions were performed using 1pmol recombinant CYP3A4 in 10 min reactions at 37ºC with 2 µM of luciferin-BE as substrate, in combination with concentrations ranging from 0.002 to 200 µM of the test thioxanthonic derivatives. CYP3A4 IC_{50} values are represented with the broken line. Values are means ± SE of three independent experiments.

To further predict the binding affinity of compounds **1** and **2** to the CYP3A4 catalytic site, a docking study using Autodock Vina was performed on those compounds, ketoconazole, a known CYP3A4 inhibitor (41) and propofol, which does not interact with CYP3A4 (29). The structure of the CYP3A4–ketoconazole is available at 3.8 Å resolution (42,43). As expected, ketoconazole registered a high affinity to the CYP3A4 catalytic site, as predicted by the highly negative docking score (Table 2). Besides, the docked ketoconazole and crystallographic ketoconazole are almost perfectly superimposed, with a RMSD of 0.14 Å. The negative control, propofol, as expected, had the worst docking score. Compounds **1-8** had docking scores ranging from -7.4 to -10.2 $kJ.mol^{-1}$, values similar to the ketoconazole control (Table 2).

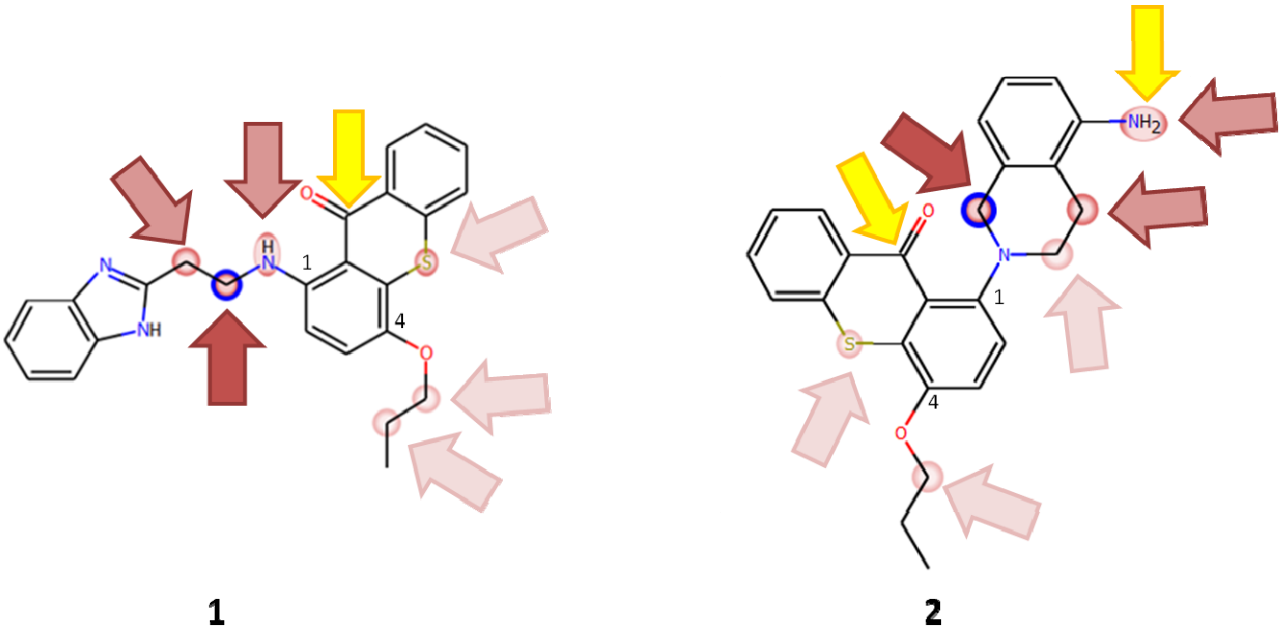

1 **2**

Figure 7. Metabolism sites and contribution: the groups in compound 1 and 2 that most likely will be metabolized by CYP3A4 are marked with dark red arrows; the darker the colour the greater the probability of metabolism occurring. The atoms in compounds 1 and 2 with the highest molecular contribution to the exposure of the metabolic "hot spot" (blue circle) to the heme moiety of CYP3A4 are marked with yellow arrows.

Table 2. (A) Docking scores obtained for test compounds **1**-**8** and controls (ketoconazole and propofol); (B) docking scores obtained for the conformations of compounds **1** and **2** in agreement with the Metasite prediction.

Scores (kJ.mol^{-1})

	A Top rank conformations	**B** Predicted by Metasite*
Ketoconazole◆	-10.8	
Compound **1**	-9.0	-8.7*
Compound **2**	-9.2	-8.3*
Compound **3**	-7.6	
Compound **4**	-8.5	
Compound **5**	-7.4	
Compound **6**	-10.2	
Compound **7**	-8.5	
Compound **8**	-9.1	
Propofol■	-5.8	

◆inhibitor of CYP3A4
■not metabolized by CYP3A4
*binding conformations represented in Figure 8

DISCUSSION

Although thioxanthones have been extensively studied for their P-gp modulation activity (10), there is a lack of more detailed information regarding their interaction with other ABC transporters. This study represents the first investigation of the potential of thioxanthonic derivatives to interact with MRP1, MRP2, MRP3, BCRP and CYP3A4.

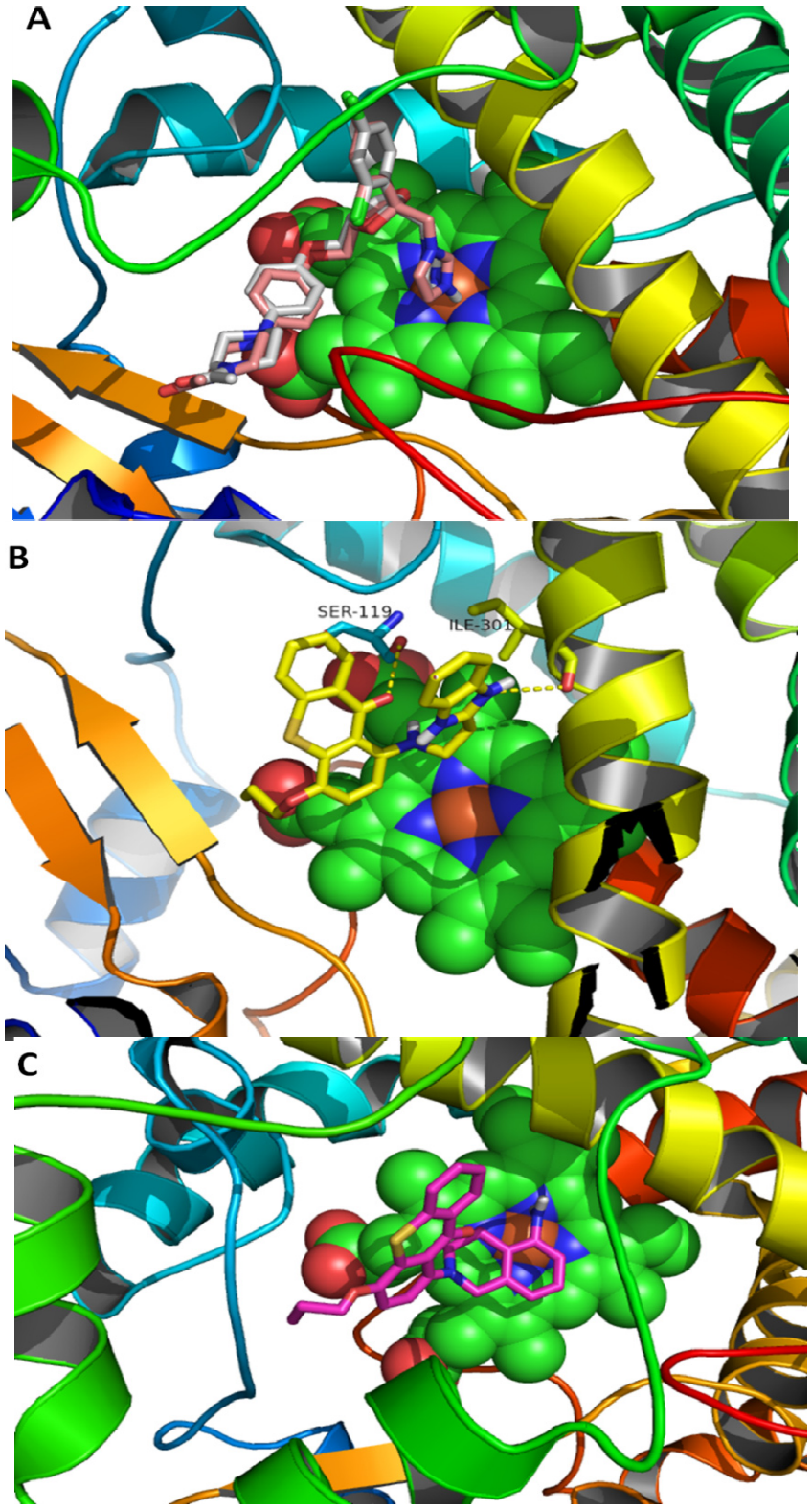

Figure 8. Representation of the crystallographic ligand ketoconazole (grey) and best docking binding conformations of the same compound (orange) (A) in CYP3A4 binding pocket. Docking conformations of compound **1** (yellow) (B) and **2** (magenta) (C) in agreement with the Metasite prediction. The heme group is represented as spheres while hydrogen bonds are represented in yellow dashes. Other noncovalent bonds were omitted for simplification.

Thioxanthones are competitive or non-competitive P-gp inhibitors

Concerning the UIC2 labelling assay, compounds **1**, **4**, **6-8** significantly decreased UIC2 reactivity, a result similar to that produced by orthovanadate, behaving as non-competitive inhibitors. On the other hand, compound **2** significantly increased UIC2 reactivity in the same order of magnitude as verapamil and quinidine, behaving as competitive inhibitors. These results are in accordance with those obtained by the luminescence-based ATPase assay(10), thereby confirming our previous data.

Thioxanthones are multi-ABC transporter inhibitors

Results regarding the effect of compound **1** on P-gp ATPase activity confirmed that compound **1** is not transported by P-gp (Figure 3A, activation study) as it does not interfere with the basal P-gp ATPase activity. Additionally, compound **1** was found to inhibit verapamil transport (Figure 3A, inhibition study) in a concentration-dependent manner up to 40 μM, before reaching a "plateau" thereafter. The IC_{50} value for inhibition of P-gp by compound **1** was close to 20 μM (Table 1). Regarding the BCRP ATPase assay, compound **1** was shown to not be a substrate for BCRP (Figure 3B, activation assay) as the levels of Pi detected were close to the baseline. Also, compound **1** inhibited the efflux of sulfasalazine (Figure 3B, inhibition assay) in a concentration-dependent manner, with an IC_{50} value of 20 μM. In addition, compound **1** was shown to be transported by MRP1 at low concentrations but at increasing concentrations (> 10 μM), the levels of transport decreased (Figure 3C, activation assay). Compound **1** also inhibited the transport of a known MRP1 substrate, NEM-GS, particularly at concentrations above 8 μM and in a concentration-dependant manner (Figure 3C, inhibition assay), presenting an IC_{50} of 25 μM. Compound **1** was a weak substrate (Figure 3D, activation assay) and weak inhibitor of sulfasalazine transport by MRP2 (Figure 3D, inhibition study). Compound **1** was revealed as a weak MPR-3 substrate at concentrations below 40 μM (Figure 3E, activation study). Compound **1** inhibited benzbromarone transport by MRP3 which only becomes more evident at concentrations above 40 μM (Figure 3E, inhibition assay), with the IC_{50} being reached only at 200 μM. Hence, compound **1** is not a substrate (or is a very low-affinity substrate) for P-gp, BCRP and MRP2 but is a substrate for MRP3 and mainly for MRP1 (as shown by values above zero in the activation studies of Figures 3C and 3E). Besides, the decreasing curves in the inhibition studies (values below 100 %) revealed that compound **1** interferes with the transport of these known ABC transporter substrates (Figure 3, inhibition studies).

The results from the effect of compound **2** on P-gp ATPase activity confirmed that compound **2** is transported by P-gp at concentrations above 10 μM (Figure 4A, activation study) and revealed that compound **2** inhibits verapamil transport at concentrations above 8 μM, in a concentration-dependent manner (Figure 4A, inhibition study). The IC_{50} value for the inhibition of P-gp by compounds **2** is close to 20 μM (Table 1). Regarding the BCRP ATPase assay, compound **2** was shown to not be a substrate for BCRP (Figure 4B, activation assay) as the levels of Pi detected were close to the baseline. In addition, compound **2** inhibited the efflux of sulfasalazine (Figure 4B, inhibition assay) in a concentration dependent manner up to concentrations of approximately 10 μM and stabilizing thereafter,, revealing an IC_{50} value of 2 μM. Compound **2** was actively transported by MRP1 at low concentrations (~1 μM) but the levels of transport decreased with increasing concentrations of this compound (Figure 4C, activation study). Indeed, data showed that compound **2** stimulated ATPase activity at low concentrations (<50 μM) but at higher concentrations (>50 μM), ATPase stimulation was found to be decreased. Compound **2** strongly inhibited the transport of NEM-GS (Figure 4C, inhibition study) with an IC_{50} of 4 μM. In addition, compound **2** was a weak MRP2 substrate (Figure 4D, activation assay) and decreased the level of Pi release to values lower than the baseline, suggesting that it blocks MRP2 basal ATPase activity at concentrations above 100 μM. Compound **2** inhibited the transport of sulfasalazine by MRP2 (Figure 4D, inhibition study), reaching the IC_{50} at 145 μM. Finally, compound **2** was transported by MRP3 but ATPase activity decreases in a concentration-dependent manner until complete loss of ATPase function becomes evident at concentrations above 100 μM (Figure 4E, activation study). Compound **2** inhibited MRP3 mediated transport of benzbromarone in a concentration-dependent manner (Figure 4E, inhibition study) with an IC_{50} value of 13 μM.

Based on the ATPase results as a whole, the IC_{50} of compounds **1** and **2** to inhibit P-gp is approximately 20 μM (for a P-gp specific substrate). However, compound **1** is also a potent BCPR and MRP1 inhibitor with IC_{50} values of 20 and 25 μM, respectively. Compound **2** is a strong

inhibitor of BCRP, MRP1 and MRP3, with IC_{50} values of 2, 4 and 13 μM, respectively.

ABC transporters are co-localized in protective tissues throughout the human body with important roles in restricting the intestinal absorption of foreign compounds and mediating the secretion of drugs and metabolites to bile (44). As a consequence, inhibition of P-gp, BCRP, and MRP1, MRP2 and MRP3 can lead to serious adverse effects, for example through the accumulation of toxic xenobiotics (45). Nonetheless, MRP1 and MRP3 are localized in basolateral membranes. P-gp, BCRP and MRP2 are localized in apical membranes. Thus, the efflux direction will be different for those pumps. For example, in an enterocyte, P-gp, BCRP, and MRP2 extrude substrates to the intestinal lumen while MRP1 and -3 pump their substrates to the systemic circulation (46,47). Besides, even if these transporters are partially blocked, other intestinal transporters such as peptide transporter 1 (PEPT1), organic anion transporters (OAT), organic cation transporters (OCT), as well as other members of the ABC family, are available for transport across the membrane (48). Therefore, as far as MDR reversal is concerned, these thioxanthonic derivatives could possibly represent further study candidates for treating cancer cells that express the ABC transporters (49). However, this could only be done by careful analysis of the phenotype of the cancer cells of each patient, using for example PET radiotracers (50).

Thioxanthones interact *in vitro* with CYP3A4

As the overlapping substrate specificity between P-gp and CYP3A4 is a common concern, namely concerning hydrophobic chemotherapeutic agents (51), the thioxanthonic derivatives **1**-**8** were screened for CYP3A4 interaction (Figure 5). CYP3A is the most prominent CYP in humans, comprising about 30 and 70% of total CYP in the liver and intestine respectively (52) and is responsible for phase I metabolism of 50% of drugs administered to humans (52). CYP3A has a very broad substrate specificity and may deactivate several anticancer drugs within the tumor cells (53).

The initial screen for CYP3A4 activity modulation demonstrated that all of the thioxanthones inhibit the metabolism of BE-luciferin by CYP3A4, reducing the production of a luciferin product that generates light when compared to the untreated control (Figure 5). Thioxanthones **1**-**8** inhibit CYP3A4 in the same order of magnitude as a known CYP3A4 inhibitor, ketoconazole (28) at the tested concentration (200 μM). Compound **1** was the compound with lower CYP3A4 inhibition ability, followed by compounds **2** and **3**. Although thioxanthones are able to inhibit several ABC transporters, their further development as clinical MDR modulators could fail due to their dose-limiting effects (54,55). Indeed, at 1-2 μM concentration (Figure 6), compounds **1** and **2** exhibit strong potency for binding CYP3A4, and activities comparable to ketoconazole in binding that enzyme (56). Thus, the competition between cytotoxic agents and these P-gp modulators for cytochrome P450 3A4 activity requires monitoring of pharmacokinetic interactions (57).

It has been previously reported that (thio)xanthonic derivatives can be substrates or inhibitors of multiple P450 isoforms (58). Therefore, the interference of compounds **1** and **2** with CYP3A4 determined experimentally using the P450-Glo kit, may result from a blockage of the CYP3A4 catalytic site or metabolism. However, this distinction would require further experiments, such as the analysis of the metabolite profile on incubation with CYP3A4 or with human liver microsomes (several CYPs) (59).

The metabolism prediction software MetaSite predicted that aliphatic carbon atoms directly linked to the nitrogen or two bonds away, the aniline, and the sulphur from the thioxanthonic ring as the most probable sites of metabolism (Figure 7). Other less relevant metabolism sites would be the carbons from the propoxy side chain (Figure 7). It may be hypothesized that the aniline will probably suffer an anilinic hydroxylation or a *N*-dealkylation and the aliphatic carbons, an aliphatic hydroxylation. The sulphur will probably be oxidized to a sulfoxide or sulfone (60).

Concerning the docking results on CYP3A4, the ketoconazole molecule has its imidazole nitrogen bound to the heme iron group (Figure 8A). The ketoconazole keto group is located in a polar pocket lined by the side chains of Arg372, Arg106 and Glu374. It has also been described that the side chain of Ser119 is important for the establishment of hydrogen bonds with some binding conformations of ketoconazole (43). Both compounds **1** and **2** are predicted to be bound in the same binding pocket as ketoconazole and with similar docking scores (Table 2). As ketoconazole, compound **1** also establishes hydrogen bounds with residue Ser119 (Figure 8B), and residue Ile301. These interactions put the "hot spot", the aliphatic carbon of the alkylarylamine, 3.0 Å from the ferryl group, in accordance with the predicted site of metabolism

for compounds **1** (Figure 7A and 8B). In an effort to arrive at a more metabolically stable compound, one could for example, modify the carbonyl group from the thioxanthone. On the other hand, compound **2** has its aniline group facing the heme group of CYP3A4 (Figure 8C). This is in accordance with the prediction which pointed to tetrahydroisoquinolinamine as the main target of metabolism (Figure 7B). Again, the carbon from thioxanthonic carbonyl on compound **2** binds non-covalently to Ser119.

Although the use of computational methods as tools for predicting the likelihood of interference with CYP3A4 are inconclusive, the study demonstrated that they could be useful in both predicting, explaining the observed data obtained from the *in vitro* experiments, and possibly guiding further molecular modifications.

CONCLUSION

Thioxanthone **1** was found to be a multi-target inhibitor of P-gp, BCRP and MRP1. Thioxanthone **2** is a multi-target inhibitor of P-gp, BCRP, MRP1 and MRP3. Therefore, they could be further tested as potential MDR reversal agents in tumor cell lines that overexpress those transporters. Further *in vivo* work should be performed to assess the toxicity of these thioxanthones. Special attention should be taken in order to avoid pharmacokinetic interactions between co-administered CYP3A4-metabolizable drugs, which could lead to increased accumulation and toxicity. Therefore, the future direction of this work will focus on the pharmacokinetic interaction between thioxanthones and anticancer agents.

ACKNOWLEDGEMENTS

This work is funded through national funds from FCT – Fundação para a Ciência e a Tecnologia under the project CEQUIMED - PEst-OE/SAU/UI4040/2011, by FEDER funds through the COMPETE program under the project FCOMP-01-0124-FEDER-011057, FCOMP-01-0124-FEDER-015752, and by U.Porto and Santander-Totta. IPATIMUP is an Associate Laboratory of the Portuguese Ministry of Science, Technology and Higher Education and is partially supported by FCT, the Portuguese Foundation for Science and Technology.

Abbreviations: ABC: ATP-binding cassette; BCRP: breast cancer resistance protein; CYP3A4: cytochrome P450 3A4; FL: fluorescence channel; MDR: multidrug resistance; MRP: multidrug resistance-associated protein; P-gp: P-glycoprotein; UIC2: P-glycoprotein monoclonal antibody.

REFERENCES

1. Goda K, Bacso Z, Szabo G. Multidrug resistance through the spectacle of P-glycoprotein. Curr Cancer Drug Targets, 2009; 9 (3): p. 281-97.
2. Yuan H, Li X, Wu J, Li J, Qu X, Xu W, et al. Strategies to overcome or circumvent P-glycoprotein mediated multidrug resistance. Curr Med Chem, 2008; 15 (5): p. 470-6.
3. Gottesman MM, Ling V. The molecular basis of multidrug resistance in cancer: the early years of P-glycoprotein research. FEBS Lett, 2006; 580 (4): p. 998-1009.
4. Ambudkar SV, Sauna ZE, Gottesman MM, Szakacs G. A novel way to spread drug resistance in tumor cells: functional intercellular transfer of P-glycoprotein (ABCB1). Trends Pharmacol Sci, 2005; 26 (8): p. 385-7.
5. Morphy R, Rankovic Z. Designing multiple ligands - medicinal chemistry strategies and challenges. Curr Pharm Des, 2009; 15 (6): p. 587-600.
6. Bailly C, Waring MJ. Preferential intercalation at AT sequences in DNA by lucanthone, hycanthone, and indazole analogs. A footprinting study. Biochemistry, 1993; 32 (23): p. 5985-93.
7. Cioli D, Pica-Mattoccia L, Archer S. Antischistosomal drugs: Past, present ... and future? Pharmacology & Therapeutics, 1995; 68 (1): p. 35-85.
8. Lockhart AC, Calvo E, Tolcher AW, Rowinsky EK, Shackleton G, Morrison JG, et al. A phase I dose-escalation study of SR271425, an intravenously dosed thioxanthone analog, administered weekly in patients with refractory solid tumors. Am J Clin Oncol, 2009; 32 (1): p. 9-14.
9. Stevenson JP, DeMaria D, Reilly D, Purvis JD, Graham MA, Lockwood G, et al. Phase I/pharmacokinetic trial of the novel thioxanthone SR233377 (WIN33377) on a 5-day schedule. Cancer Chemother Pharmacol, 1999; 44 (3): p. 228-34.
10. Palmeira A, Vasconcelos MH, Paiva A, Fernandes MX, Pinto MM, Sousa E. Dual inhibitors of P-glycoprotein and tumor cell growth: (re)discovering thioxanthones. Biochem Pharmacol, 2012; 83 (1): p. 57-68.
11. Goncalves PH, High F, Juniewicz P, Shackleton G, Li J, Boerner S, et al. Phase I dose-escalation study of the thioxanthone SR271425 administered intravenously once every 3 weeks in patients with advanced malignancies. Invest New Drugs, 2008; 26 (4): p. 347-54.
12. McDevitt CA, Callaghan R. How can we best use structural information on P-glycoprotein to design inhibitors? Pharmacology & Therapeutics, 2007; 113 (2): p. 429-41.

13. Leslie EM, Deeley RG, Cole SP. Multidrug resistance proteins: role of P-glycoprotein, MRP1, MRP2, and BCRP (ABCG2) in tissue defense. Toxicol Appl Pharmacol, 2005; 204 (3): p. 216-37.
14. Kannan P, Telu S, Shukla S, Ambudkar SV, Pike VW, Halldin C, et al. The "Specific" P-Glycoprotein Inhibitor Tariquidar Is Also a Substrate and an Inhibitor for Breast Cancer Resistance Protein (BCRP/ABCG2). ACS Chemical Neuroscience, 2011; 2 (2): p. 82-9.
15. Robey RW, Shukla S, Finley EM, Oldham RK, Barnett D, Ambudkar SV, et al. Inhibition of P-glycoprotein (ABCB1)- and multidrug resistance-associated protein 1 (ABCC1)-mediated transport by the orally administered inhibitor, CBT-1((R)). Biochem Pharmacol, 2008; 75 (6): p. 1302-12.
16. Boumendjel A, Baubichon-Cortay H, Trompier D, Perrotton T, Di Pietro A. Anticancer multidrug resistance mediated by MRP1: recent advances in the discovery of reversal agents. Med Res Rev, 2005; 25 (4): p. 453-72.
17. Nabekura T, Yamaki T, Ueno K, Kitagawa S. Inhibition of P-glycoprotein and multidrug resistance protein 1 by dietary phytochemicals. Cancer Chemother Pharmacol, 2008; 62 (5): p. 867-73.
18. Sun M, Xu X, Lu Q, Pan Q, Hu X. Schisandrin B: a dual inhibitor of P-glycoprotein and multidrug resistance-associated protein 1. Cancer Lett, 2007; 246 (1-2): p. 300-7.
19. Wang S, Ryder H, Pretswell I, Depledge P, Milton J, Hancox TC, et al. Studies on quinazolinones as dual inhibitors of Pgp and MRP1 in multidrug resistance. Bioorg Med Chem Lett, 2002; 12 (4): p. 571-4.
20. Shukla S, Wu CP, Ambudkar SV. Development of inhibitors of ATP-binding cassette drug transporters: present status and challenges. Expert Opin Drug Metab Toxicol, 2008; 4 (2): p. 205-23.
21. Nagy H, Goda K, Arceci R, Cianfriglia M, Mechetner E, Szabo G, Jr. P-Glycoprotein conformational changes detected by antibody competition. Eur J Biochem, 2001; 268 (8): p. 2416-20.
22. Palmeira A, Rodrigues F, Sousa E, Pinto M, Vasconcelos MH, Fernandes MX. New uses for old drugs: pharmacophore-based screening for the discovery of P-glycoprotein inhibitors. Chem Biol Drug Des, 2011; 78 (1): p. 57-72.
23. Glavinas H, Kis E, Pal A, Kovacs R, Jani M, Vagi E, et al. ABCG2 (breast cancer resistance protein/mitoxantrone resistance-associated protein) ATPase assay: a useful tool to detect drug-transporter interactions. Drug Metab Dispos, 2007; 35 (9): p. 1533-42.
24. Mehn D. Determination of the interaction of drugs with the human MDR1 transporter using the SB-MDR1 PREDEASYTM ATPase Kit. Solvo Biotech, 2007; 1.2: p. 1-19.
25. Oosterhuis B, Vukman K, Vagi E, Glavinas H, Jablonkai I, Krajcsi P. Specific interactions of chloroacetanilide herbicides with human ABC transporter proteins. Toxicology, 2008; 248 (1): p. 45-51.
26. Froimowitz M. HyperChem: a software package for computational chemistry and molecular modeling. Biotechniques, 1993; 14 (6): p. 1010-3.
27. Cruciani G, Carosati E, De Boeck B, Ethirajulu K, Mackie C, Howe T, et al. MetaSite: understanding metabolism in human cytochromes from the perspective of the chemist. J Med Chem, 2005; 48 (22): p. 6970-9.
28. Usmani KA, Tang J. Human cytochrome P450: metabolism of testosterone by CYP3A4 and inhibition by ketoconazole. Curr Protoc Toxicol, 2004; Chapter 4: p. Unit4 13.
29. Oda Y, Hamaoka N, Hiroi T, Imaoka S, Hase I, Tanaka K, et al. Involvement of human liver cytochrome P4502B6 in the metabolism of propofol. Br J Clin Pharmacol, 2001; 51 (3): p. 281-5.
30. Trott O, Olson AJ. AutoDock Vina: improving the speed and accuracy of docking with a new scoring function, efficient optimization, and multithreading. J Comput Chem, 2009; 31 (2): p. 455-61.
31. Park SW, Lomri N, Simeoni LA, Fruehauf JP, Mechetner E. Analysis of P-glycoprotein-mediated membrane transport in human peripheral blood lymphocytes using the UIC2 shift assay. Cytometry A, 2003; 53 (2): p. 67-78.
32. Mechetner EB, Schott B, Morse BS, Stein WD, Druley T, Davis KA, et al. P-glycoprotein function involves conformational transitions detectable by differential immunoreactivity. Proc Natl Acad Sci U S A, 1997; 94 (24): p. 12908-13.
33. Zhou Y, Gottesman MM, Pastan I. The extracellular loop between TM5 and TM6 of P-glycoprotein is required for reactivity with monoclonal antibody UIC2. Arch Biochem Biophys, 1999; 367 (1): p. 74-80.
34. Sauna ZE, Ambudkar SV. About a switch: how P-glycoprotein (ABCB1) harnesses the energy of ATP binding and hydrolysis to do mechanical work. Mol Cancer Ther, 2007; 6 (1): p. 13-23.
35. Kis E, Nagy T, Jani M, Molnar E, Janossy J, Ujhellyi O, et al. Leflunomide and its metabolite A771726 are high affinity substrates of BCRP: implications for drug resistance. Ann Rheum Dis, 2009; 68 (7): p. 1201-7.
36. Sarkadi B, Price EM, Boucher RC, Germann UA, Scarborough GA. Expression of the human multidrug resistance cDNA in insect cells generates a high activity drug-stimulated membrane ATPase. J Biol Chem, 1992; 267 (7): p. 4854-8.
37. Pal A, Mehn D, Molnar E, Gedey S, Meszaros P, Nagy T, et al. Cholesterol potentiates ABCG2 activity in a heterologous expression system: improved in vitro model to study function of human ABCG2. J Pharmacol Exp Ther, 2007; 321 (3): p. 1085-94.
38. Promega. P450-Glo™ Assays - Technical bulletin; http://www.promega.com/tbs/tb325/tb325.pdf (accessed on March 2011).

39. Cali J. Screen for CYP3A4 inhibitors using P450-Glo luminescent cytochrome P450 assays. Cell notes, 2003; (7): p. 2-4.
40. Shin Y, Le H, Khojasteh C, Hop CE. Comparison of Metabolic Soft Spot Predictions of CYP3A4, CYP2C9 and CYP2D6 Substrates Using MetaSite and StarDrop. Comb Chem High Throughput Screen, 2011: p.
41. Gibbs MA, Baillie MT, Shen DD, Kunze KL, Thummel KE. Persistent inhibition of CYP3A4 by ketoconazole in modified Caco-2 cells. Pharm Res, 2000; 17 (3): p. 299-305.
42. Ekroos M, Sjogren T. Structural basis for ligand promiscuity in cytochrome P450 3A4. Proc Natl Acad Sci U S A, 2006; 103 (37): p. 13682-7.
43. Ekins S, Stresser DM, Williams JA. In vitro and pharmacophore insights into CYP3A enzymes. Trends Pharmacol Sci, 2003; 24 (4): p. 161-6.
44. Ueda K. ABC Proteins Protect the Human Body and Maintain Optimal Health. Biosci Biotechnol Biochem, 2011: p.
45. Hoffmann U, Kroemer HK. The ABC transporters MDR1 and MRP2: multiple functions in disposition of xenobiotics and drug resistance. Drug Metab Rev, 2004; 36 (3-4): p. 669-701.
46. Krishnamurthy P, Schuetz JD. Role of ABCG2/BCRP in biology and medicine. Annu Rev Pharmacol Toxicol, 2006; 46: p. 381-410.
47. Kruh GD, Belinsky MG. The MRP family of drug efflux pumps. Oncogene, 2003; 22 (47): p. 7537-52.
48. Zair ZM, Eloranta JJ, Stieger B, Kullak-Ublick GA. Pharmacogenetics of OATP (SLC21/SLCO), OAT and OCT (SLC22) and PEPT (SLC15) transporters in the intestine, liver and kidney. Pharmacogenomics, 2008; 9 (5): p. 597-624.
49. Cuestas ML, Sosnik A, Mathet V. Poloxamines display a multiple inhibitory activity of ATP-Binding Cassette (ABC) transporters in cancer cell lines. Mol Pharm, 2011: p.
50. Bankstahl JP, Kuntner C, Abrahim A, Karch R, Stanek J, Wanek T, et al. Tariquidar-induced P-glycoprotein inhibition at the rat blood-brain barrier studied with (R)-11C-verapamil and PET. J Nucl Med, 2008; 49 (8): p. 1328-35.
51. Guns ES, Bullock PL, Reimer ML, Dixon R, Bally M, Mayer LD. Assessment of the involvement of CYP3A in the vitro metabolism of a new modulator of MDR in cancer chemotherapy, OC144-193, by human liver microsomes. Eur J Drug Metab Pharmacokinet, 2001; 26 (4): p. 273-82.
52. Guengerich FP. Cytochrome P-450 3A4: regulation and role in drug metabolism. Annu Rev Pharmacol Toxicol, 1999; 39: p. 1-17.
53. Wacher VJ, Wu CY, Benet LZ. Overlapping substrate specificities and tissue distribution of cytochrome P450 3A and P-glycoprotein: implications for drug delivery and activity in cancer chemotherapy. Mol Carcinog, 1995; 13 (3): p. 129-34.
54. Gottesman MM, Fojo T, Bates SE. Multidrug resistance in cancer: role of ATP-dependent transporters. Nat Rev Cancer, 2002; 2 (1): p. 48-58.
55. Schinkel AH, Jonker JW. Mammalian drug efflux transporters of the ATP binding cassette (ABC) family: an overview. Adv Drug Deliv Rev, 2003; 55 (1): p. 3-29.
56. Dvorak Z. Drug-drug interactions by azole antifungals: Beyond a dogma of CYP3A4 enzyme activity inhibition. Toxicol Lett, 2011; 202 (2): p. 129-32.
57. Thomas H, Coley HM. Overcoming multidrug resistance in cancer: an update on the clinical strategy of inhibiting p-glycoprotein. Cancer Control, 2003; 10 (2): p. 159-65.
58. Foti RS, Pearson JT, Rock DA, Wahlstrom JL, Wienkers LC. In vitro inhibition of multiple cytochrome P450 isoforms by xanthone derivatives from mangosteen extract. Drug Metab Dispos, 2009; 37 (9): p. 1848-55.
59. Natsui K, Mizuno Y, Tani N, Yabuki M, Komuro S. Identification of CYP3A4 as the primary cytochrome P450 responsible for the metabolism of tandospirone by human liver microsomes. Eur J Drug Metab Pharmacokinet, 2007; 32 (4): p. 233-40.
60. Guengerich FP. Cytochrome p450 and chemical toxicology. Chem Res Toxicol, 2008; 21 (1): p. 70-83.